Advances in Nano Research, *Vol. 11, No. 2 (2021) 193-201*
https://doi.org/10.12989/anr.2021.11.2.193

An investigation of mechanical properties of kidney tissues by using mechanical bidomain model

Muhammad Taj[1], Mohamed A. Khadimallah[2,3], Muzamal Hussain*[4], Mohamed Elbahar[2], Monzoor Ahmad[1], Elaloui Elimame[5], Shakeel ul Zaman[1] and Abdelouahed Tounsi[6,7]

[1]*Department of Mathematics, University of Azad Jammu and Kashmir, Muzaffarabad, 1300, Azad Kashmir, Pakistan*
[2]*Prince Sattam Bin Abdulaziz University, College of Engineering, Civil Engineering Department, Al-Kharj, 16273, Saudi Arabia*
[3]*Laboratory of Systems and Applied Mechanics, Polytechnic School of Tunisia, University of Carthage, Tunis, Tunisia*
[4]*Department of Mathematics, Govt. College University Faisalabad, 38000, Faisalabad, Pakistan*
[5]*Laboratory of Materials Applications in Environment, Water and Energy LR21ES15, Faculty of Sciences, University of Gafsa, Tunisia*
[6]*YFL (Yonsei Frontier Lab), Yonsei University, Seoul, Korea*
[7]*Department of Civil and Environmental Engineering, King Fahd University of Petroleum & Minerals, 31261 Dhahran, Eastern Province, Saudi Arabia*

(*Received February 26, 2021, Revised June 24, 2021, Accepted July 6, 2021*)

Abstract. In this study, mechanical bidomain model is used to study the mechanical behavior of kidney tissues. This model has been used widely to study cardiac tissue and cell colony. On recognizing same structural and somehow same physiological relationship between cardiac tissue and kidney tissue, the displacements in different regions of kidney and the integrins, i. e., nephron coupling the intracellular medulla and extracellular cortex is analyzed. The mechanical Bidomain model provides a microscopic description of kidney tissue mechanics and also predicts the microscopic coupling of extracellular cells region of kidney tissue, i.e., cortex and the intracellular cells region medulla of kidney.

Keywords: extracellular cortex; intracellular medulla; kidney tissues; mechanical bidomain model

1. Introduction

The anisotropic electrical properties of cardiac tissues were represented mathematically by Bi domain model. Actually by domain model is developed using realistic physiological parameter values based on experimental measurement. The pinor of Bidomain model is (Leibovic 2013). After this (Roth 1992, Tung 1978, Geselowitz and Miller 1983) made further developments in the Bidomain model and these developments were used by Roth (2013) and Sepulveda *et al.* (1989). The mechanism and practical implication of Bi-domain model was recently used by many researchers to develop the microscopic properties of cardiac muscle cells. Roth (2013), Henriquez and Ying (2009) and Trayanova and Plank (2009) used this model for the mechanical Bi-domain model for the description of elastic behavior of cardiac tissues.

Neu and Krassowska (1993) first derived reaction diffusion equation for the microstructure and basic physical principles and conclude that Bi-domain model is the special case of reaction diffusion equation. Bi-domain model is used to approximate the average electrical behaviors of cells in the colony rather than as a single cell. Hence the nature of the Bi-domain model is continuum. In carrying out the analysis by Bi-domain model the micro structure of cardiac tissue is replaced by intracellular and extracellular continua and each filling of space occupied by the actual tissue also if we consider the effect of bath stimuli and conductivity tensor to make the tissue anisotropic. Trayanova *et al.* (2006) and Pathmanathan *et al*. (2010) use Bidomain model for the simulation for the injection current where the extracellular space exist cathode and hyperpolarized it along the direction of the fibers. The regions of depolarization and hyperpolarization are called the virtual cathode and virtual anode was described by Wikswo Jr *et al.* (1995) and Neunlist and Tung (1995). The boundary conditions at the interface between cardiac tissue and adjacent conductors were stimulated by Krassowska and Neu (1994). Three boundary conditions are applied at tissue electrode interface the normal component of the intercellular current density is considered to be zero.

Akbaş (2016a, b) studied the forced vibration analysis of a simple supported viscoelastic nanobeam based on modified couple stress theory (MCST). The nanobeam is excited by a transverse triangular force impulse modulated by a harmonic motion. The elastic medium is considered as Winkler-Pasternak elastic foundation. The damping effect is considered by using the Kelvin–Voigt viscoelastic model. The cracked beam is modelled using a proper modification of the classical cracked-beam theory consisting of two sub-beams connected through a massless elastic rotational spring.

Krassowska and Neu (1994) defined the boundary conditions when the extracellular potential is constant and

*Corresponding author, Ph.D.,
E-mail: muzamal45@gmail.com;
muzamalhussain@gcuf.edu.pk

ISSN: 2287-237X (Print), 2287-2388 (Online)

total current passing from the electrode into extra cellular space is equal to the stimulus current. Roth (2013) developed a mechanical Bidomain model in which he found the mechanisms by which cell convert mechanical stimuli into cell growth, mechanotransduction and remodeling. Akbaş (2018c) presented the forced vibration responses of a cantilever nanobeam with crack using modified couple stress theory with damping effect. The crack is modeled with a rotational spring. The Kelvin–Voigt model is considered in the damping effect. In solution of the dynamic problem, finite element method is used within Timoshenko beam theory in the time domain. Influences of the geometry, crack and material parameters on forced vibration responses of cracked nanobeams are examined and discussed.

Sharma and Roth (2014) analysis the influence of compressibility on the mechanical Bidomain model in the analysis they found that there is a microscopic pressure difference between the intracellular and extracellular spaces in the domain. Puwal and Roth (2010) use the electrical Bidomain model for cardiac tissue instead of Monodomain model they found pressure and displacement by considering intracellular and extracellular spaces separately.

Akbaş (2017a, b) investigated the forced vibration analysis of a cracked functionally graded microbeam using modified couple stress theory with damping effect. Mechanical properties of the functionally graded beam change vary along the thickness direction. The crack is modelled with a rotational spring. The Kelvin-Voigt model is considered in the damping effect. static bending of an edge cracked cantilever nanobeam composed of functionally graded material (FGM) subjected to transversal point load at the free end of the beam is investigated based on modified couple stress theory. Material properties of the beam change in the height direction according to exponential distributions. Civalek *et al*. (2021) presented the free vibration behavior of carbon nanotube-reinforced composite (CNTRC) microbeams is investigated. Carbon nanotubes (CNTs) are distributed in a polymeric matrix with four different patterns of the reinforcement. The material properties of the CNTRC microbeams are predicted by using the rule of mixture.

Karami and Janghorban (2020) proposed a non-classical quasi three-dimensional shell theory to analyze the static phenomenon of doubly-curved nanoshells whose made of functionally graded (FG) anisotropic material. The mechanical properties vary exponentially via the z-axis. Compared to other shell theories, the proposed model needs only seven unknown variables to determine fourfold coupled (axial-shear-bending-stretching) static and buckling responses.

Roth and Basser (2009) use the theories of electromagnetism and electricity to predict the displacement to describe the Lerentz force. Roth (2013) use the monodomain model to study the elastic property of cardiac tissue he found that the boundary layers arises due to redistribution of stresses in the intracellular and extracellular displacements in order to make the normal stresses in both spaces. Roth (2016) made a mathematical analysis how the extracellular matrix and intracellular cytoskeleton are connected by integrin proteins. He suggests that Bidomain model may be applicable to cardiac remodeling, blood vessel regulation, and tissue engraining and cancer biology. Noroozi *et al*. (2020) studied for the first time based on the nonlocal strain gradient theory the effect of size dependency in torsional vibration of bi-direction functionally graded (FG) nonlinear nano-cone. The material properties were assumed to vary according to the arbitrary function in radial and axial directions. Roth (1991) used the Bidomain model to present the electrical properties of tissues and Ebihara-Johnson model is used to represent the properties of active sodium channel. Roth (1996) predict the complex anodal and cathodal strength interval curves by using Bidomain model his result show a great resemblance with the experimental observation of Gonzalez-Rosende *et al*. (1988). He used the finite element method to solve the bidomain equation which is molded by two dimensional sheet of anisotropic cardiac tissue they found that the current injected into the tissue at cathode produced both depolarization and hyperpolarization. The response of spherical heart to a uniform electric field by using bidomain model is stimulated by Trayanova *et al*. (1993) find the magnetic field and its influence on MRI use the spherical coordinates to find the magnetic field. Eaton (1992) viewed the basic principle of magnetic simulation of biological tissues in certain pathologic conditions their result demonstrate the potential for reorganization in motor system in peripheral as well as in the control neveral system. Akbaş (2017a, b) investigated the free vibration analysis of edge cracked cantilever microscale beams composed of functionally graded material (FGM) based on the modified couple stress theory (MCST). The material properties of the beam are assumed to change in the height direction according to the exponential distribution. The FG nanobeam is excited by a transverse triangular force impulse modulated by a harmonic motion. Mechanical properties of FG beam depends on the position. The Kelvin–Voigt model is considered in the damping effect. In solution of the dynamic problem, finite element method is used within Timoshenko beam theory. Galappaththige *et al*. (2017) study the cardiac tissue which is electrically conducted by a unipolar electrode numerical simulation predicts that around an electrode adjacent region of depolarization and hyperpolarization exist. Nejadi and Mohammadimehr (2020) studied the buckling analysis of sandwich composite (carbon nanotube reinforced composite and fiber reinforced composite) Euler-Bernoulli beam in two configurations (core and layers material), three laminates (combination of different angles) and two models (relative thickness of core according to peripheral layers) using differential quadrature method (DQM) is studied. Roth (2013) viewed the elastic deformation of cardiac tissue under an applied stress he notice that the permitting shear waves propagate through the heart. This behavior is modeled by a monodomain approach, but they consider the Bidomain model of cardiac tissue. They found the two normal modes of oscillation one is monodomain mode and other is Bidomain mode. Recently some researcher used different methods for nonlinear modeling (Eltaher *et al.* 2019, Ebrahimi *et al*. 2019, Safaei *et al*. 2019, Shahsavari *et*

al. 2019, Benmansour *et al*. 2019, Arefi and Zur 2020, Zhou *et al.* 2020, Nazemnezhad and Shokrollahi *et al*. 2020). Prior and Roth (2008) view the effect of electric current on the transmambrane potential as a shock is applied to heart. They combine the Bidomain equations along the photon diffusion equation to study the excitation and emission of photons during the optical mapping of cardiac tissue. They used imaging method to accurately reconstruct transmembrane potential. Roth (2013) use the mechanical Bidomain model to describe a two dimensional sheet of cardiac tissue undergoing a uniform active tension. At the boundary, the tissue sheet is free to move. He found the analytical solution for the intracellular and extracellular displacement and pressure.

2. Methodology

Mechanical Bidomain model is used to study the mechanical behavior of kidney tissues. This model has been used widely to study cardiac tissue and cell colony. On recognizing same structural and somehow same physiological relationship between cardiac tissue and kidney tissue, auther tried to analyze the displacements in different regions of kidney and the integrin's.

3. Mathematical formulation of problem

3.1 Stress for inner region

The internal region of kidney is renal medulla and the stress (τ_i) is named as intracellular stress. Mainly this stress is caused by intracellular hydrostatic pressure (p), Isotropic shear stress which is proportional to shear modulus (ν) and intracellular shear strain (ε_1). Anisotropic Young modulus with the medullanal fiber (λ). Tension acting with fibers (T). So for two dimensional case the intracellular stress tensor contain three terms: τ_{ixx}, τ_{iyy} and τ_{ixy}.

$$\tau_{ixx} = -p + 2\upsilon\varepsilon_{ixx} + \gamma\varepsilon_{ixx} + T \tag{1}$$

$$\tau_{iyy} = -p + 2\upsilon\varepsilon_{iyy}. \tag{2}$$

$$\tau_{ixy} = 2\upsilon\varepsilon_{ixy}. \tag{3}$$

3.2 Stress for outer region

The outer region of kidney is renal cortex and the stresses for this region are termed as extracellular stresses. For extracellular surface, the extracellular stress having two terms, the extracellular hydrostatic pressure (q) and isotropic shear stress which is proportional to the extracellular shear strain (ε_e) with shear modulus (μ). So for two dimensional case the extracellular stress tensor also contain three terms: τ_{exx}, τ_{eyy} and τ_{exy}.

$$\tau_{exx} = -q + 2\mu\varepsilon_{exx} \tag{4}$$

$$\tau_{eyy} = -q + 2\mu\varepsilon_{eyy}. \tag{5}$$

$$\tau_{exy} = 2\mu\varepsilon_{exy} \tag{6}$$

3.3 Stress and displacement relationship for inner region

$$\varepsilon_{ixx} = \frac{\partial u_x}{\partial x}, \varepsilon_{iyy} = \frac{\partial u_y}{\partial y}, \varepsilon_{ixy} = \frac{1}{2}\left(\frac{\partial u_x}{\partial y} + \frac{\partial u_y}{\partial x}\right) \tag{7}$$

where u_x, u_y and u_z are components of displacements for intracellular space. The intracellular space is incompressible so the displacement can be obtained from the intracellular stream functions.

$$u_x = \frac{\partial \phi}{\partial y}, u_y = -\frac{\partial \phi}{\partial x} \tag{8}$$

3.4 Stress and displacement relationship for outer region

$$\varepsilon_{exx} = \frac{\partial w_x}{\partial x}, \varepsilon_{eyy} = \frac{\partial w_y}{\partial y}, \varepsilon_{exy} = \frac{1}{2}\left(\frac{\partial w_x}{\partial y} + \frac{\partial w_y}{\partial x}\right) \tag{9}$$

where w_x, w_y and w_z are the components of displacement for extracellular space. The extracellular space is incompressible so the displacement can be obtained from the extracellular stream functions. i.e.,

$$w_x = \frac{\partial \eta}{\partial y}, w_y = -\frac{\partial \eta}{\partial x}. \tag{10}$$

3.5 Equations of equilibrium for inner region

These equations consist of taking the divergence of intracellular stress tensors and adding a terms show a coupling of intracellular space via a spring constant.

$$\frac{\partial \tau_{ixx}}{\partial x} + \frac{\partial \tau_{ixy}}{\partial y} = K(u_x - w_x) \tag{11}$$

$$\frac{\partial \tau_{ixy}}{\partial x} + \frac{\partial \tau_{iyy}}{\partial y} = K\left(u_y - w_y\right) \tag{12}$$

where K is known as a spring constant and it represent an integrin protein and $u - w$ show a coupling between a displacement of intracellular and extracellular spaces.

3.6 Equations of equilibrium for outer region

These equations consist of taking the divergence of extracellular stress tensors and adding the terms, show a coupling of extracellular space via a spring constant.

$$\frac{\partial \tau_{exx}}{\partial x} + \frac{\partial \tau_{exy}}{\partial y} = -K\,(u_x - w_x) \tag{13}$$

$$\frac{\partial \tau_{exy}}{\partial x}+\frac{\partial \tau_{eyy}}{\partial y}=-K\left(u_y-w_y\right) \tag{14}$$

where K is known as a spring constant and it represent an integrin protein and $u-w$ show a coupling between a displacement of intracellular and extracellular spaces.

4.Derivation of bidomain model

After defining shear stresses, shear strain, displacement stress relation and Equilibrium equation for two regions we derive the mechanical bidomain model as:

Using Eqs. (1) and (3) in Eq. (11) we get

$$\begin{aligned}\frac{-\partial p}{\partial x}+2\upsilon\frac{\partial}{\partial x}(\varepsilon_{ixx})+\ \gamma\frac{\partial}{\partial x}(\varepsilon_{ixx})+2\upsilon\frac{\partial}{\partial y}\left(\varepsilon_{ixy}\right)\\ =\mathrm{K}\left(u_x-w_x\right)\end{aligned} \tag{15}$$

Now using Eqs. (7), (8) and (10) in Eq. (15) we get

$$\begin{aligned}&\frac{-\partial p}{\partial x}+\upsilon\left(\frac{\partial^3\phi}{\partial x^2\partial y}+\frac{\partial^3\phi}{\partial y^3}\right)+\gamma\frac{\partial^3\phi}{\partial x^2\partial y}+\frac{\partial T}{\partial x}\\ &=K\left(\frac{\partial\phi}{\partial y}+\frac{\partial\eta}{\partial y}\right)\end{aligned} \tag{16}$$

Similarly using Eqs. (2), (3) and (1) in Eq. (12) we get

$$\begin{aligned}&\frac{-\partial p}{\partial y}+2\upsilon\frac{\partial}{\partial x}\left(\varepsilon_{ixy}\right)+\ 2\upsilon\frac{\partial}{\partial x}\left(\varepsilon_{iyy}\right)+2\vartheta\frac{\partial}{\partial y}\left(\varepsilon_{ixy}\right)\\ &=\mathrm{K}\left(u_y-w_y\right)\end{aligned} \tag{17}$$

Now using Eqs. (7), (8) and (10) in equation (17) we get

$$\frac{-\partial p}{\partial y}-\upsilon\left(\frac{\partial^3\phi}{\partial x\partial y^2}+\frac{\partial^3\phi}{\partial x^3}\right)=-\mathrm{K}\left(\frac{\partial\phi}{\partial y}-\frac{\partial\eta}{\partial y}\right) \tag{18}$$

Eqs. (17) and (18) are known as Bi domain equations for intracellular space.

Similarly to get a Bi domain equation for extracellular space we use same procedure which is used to get a Bi domain equation for intracellular region.

Using Eqs. (4) and (6) in Eq. (13) we get.

$$\frac{-\partial q}{\partial x}+2\mu\frac{\partial}{\partial x}\left(\varepsilon_{exx}\right)+2\mu\frac{\partial}{\partial y}\left(\varepsilon_{exy}\right)=-\mathrm{K}\left(u_x-w_x\right) \tag{19}$$

Now using Eqs. (8), (9) and (10) in Eq. (19) we get.

$$\frac{-\partial q}{\partial x}+\mu\left(\frac{\partial^3\eta}{\partial x^2\partial y}+\frac{\partial^3\eta}{\partial y^3}\right)=-\mathrm{K}\left(\frac{\partial\phi}{\partial y}-\frac{\partial\eta}{\partial y}\right) \tag{20}$$

Similarly using Eqs. (5) and (6) in Eq. (14) we get

$$\frac{-\partial q}{\partial y}+2\mu\frac{\partial}{\partial x}\left(\varepsilon_{exy}\right)+2\mu\frac{\partial}{\partial y}\left(\varepsilon_{eyy}\right)=-\mathrm{K}\left(u_y-w_y\right) \tag{21}$$

Now using Eqs. (8)-(10) in Eq. (17) we get

$$\frac{-\partial q}{\partial y}-\mu\left(\frac{\partial^3\eta}{\partial x\partial y^2}+\frac{\partial^3\eta}{\partial x^3}\right)=-\mathrm{K}\left(\frac{\partial\phi}{\partial x}-\frac{\partial\eta}{\partial x}\right) \tag{22}$$

Eqs. (20) and (22) are known as Bi domain equations for extracellular region.

4.1 Solution of bidomain equations

The solution of Bidomain equations can be obtained by using analytical and numerical techniques. In our problem we use analytical technique to solve the problem by using appropriate boundaries conditions.

Now we guessed the solution which contains several unknown constant parameters. We assumed an analytical solution of differential equations. Our guessed solutions are as:

$$\phi=Ay^2+B\cosh\left(\frac{y}{\sigma}\right),\qquad p=0, \tag{23}$$

$$\eta=Cy^2+D\cosh\left(\frac{y}{\sigma}\right),\qquad q=0. \tag{24}$$

where in Eqs. (23) and (24) unknown constant parameters are A,B,C,D and σ. These solutions have hyperbolic cosine function. If $\sigma<<L$ at the tissue surface $y=L$ the hyperbolic cosine function behaves like an exponential function.

Now differentiating Eq. (23) with respect to *x* and *y* the resulting form is

$$\frac{\partial\phi}{\partial x}=0,\frac{\partial\phi}{\partial y}=2Ay+\frac{B}{\sigma}\sin h\left(\frac{y}{\sigma}\right) \tag{25}$$

Now again differentiating Eq. (25) with respect to *x* and *y* the resulting form is

$$\frac{\partial^2\phi}{\partial x^2}=0,\frac{\partial^2\phi}{\partial y^2}=2A+\frac{B}{\sigma^2}\cos h\left(\frac{y}{\sigma}\right) \tag{26}$$

And also

$$\frac{\partial^3\phi}{\partial y^3}=\frac{B}{\sigma^3}\sin h\left(\frac{y}{\sigma}\right),\frac{\partial^2\phi}{\partial x^2\partial y}=0 \tag{27}$$

Now differentiating Eq. (24) with respect to *x* and *y* the resulting form is

$$\frac{\partial\eta}{\partial x}=0,\frac{\partial\eta}{\partial y}=2C+\frac{D}{\sigma^2}\cos h\left(\frac{y}{\sigma}\right) \tag{28}$$

Now again differentiating Eq. (27) with respect to *x* and *y* the resulting form is

$$\frac{\partial^2\eta}{\partial x^2}=0,\qquad\frac{\partial^2\eta}{\partial y^2}=2C+\frac{D}{\sigma^2}\cos h\left(\frac{y}{\sigma}\right) \tag{29}$$

And also

$$\frac{\partial^3\eta}{\partial y^3}=\frac{D}{\sigma^3}\sin h\left(\frac{y}{\sigma}\right),\qquad\frac{\partial^2\eta}{\partial x^2\partial y}=0 \tag{30}$$

Putting Eqs. (25)-(27) in Eq. (16) we get

$$\begin{aligned}&\frac{-\partial(0)}{\partial x}+\upsilon\left(0+\frac{B}{\sigma^3}\sin h\left(\frac{y}{\sigma}\right)\right)+\gamma(0)+\frac{\partial T}{\partial x}\\ &=K\left(2Ay+\frac{B}{\sigma}\sin h\left(\frac{y}{\sigma}\right)\ -2Cy-\frac{D}{\sigma}\sin h\left(\frac{y}{\sigma}\right)\right)\\ &\frac{B\upsilon}{\sigma^3}\sin h\left(\frac{y}{\sigma}\right)+\frac{\partial T}{\partial x}\\ &=K\left(2Ay+\frac{B}{\sigma}\sin h\left(\frac{y}{\sigma}\right)\ -2Cy-\frac{D}{\sigma}\sin h\left(\frac{y}{\sigma}\right)\right)\end{aligned}$$

As active tension assumed to zero so, $\frac{\partial T}{\partial x} = 0$.

$$\frac{B\upsilon}{\sigma^3}\sin h\left(\frac{y}{\sigma}\right) = K\left(2Ay + \frac{B}{\sigma}sin\ h\left(\frac{y}{\sigma}\right) - 2Cy - \frac{D}{\sigma}sin\ h\left(\frac{y}{\sigma}\right)\right) \quad (31)$$

Similarly putting Eqs. (25)-(27) in Eq. (18) we get.

$$\frac{-\partial(0)}{\partial y} - \upsilon(0+0\ ) = -K(0\ -0)$$

The Eq. (18) is identically satisfied.

Putting Eqs. (28)-(30) in Eq. (20) we get.

$$\frac{-\partial(0)}{\partial x} + \mu\left(0 + \frac{D}{\sigma^3}sin\ h\left(\frac{y}{\sigma}\right)\right) = -\mathrm{K}\left(2A + \frac{B}{\sigma^2}cos\ h\left(\frac{y}{\sigma}\right) - 2C - \frac{D}{\sigma^2}cos\ h\left(\frac{y}{\sigma}\right)\right) \quad (32)$$

$$\frac{\mu D}{\sigma^3}\sin h\left(\frac{y}{\sigma}\right) = -\mathrm{K}\left(2A + \frac{B}{\sigma^2}cos\ h\left(\frac{y}{\sigma}\right) - 2C - \frac{D}{\sigma^2}cos\ h\left(\frac{y}{\sigma}\right)\right)$$

Similarly putting Eqs. (28)-(30) in Eq. (32) we get.

$$\frac{-\partial(0)}{\partial y} - \mu(0+0) = -\mathrm{K}\,(0-0)$$

The Eq. (32) is also identically satisfied.

In order to satisfy the Eqs. (31) and (32) for all values of y the parameters are related to each other by.

$$C = A.\ D = -\upsilon\mu B \text{ and } \sigma = \upsilon\mu K(\upsilon+\mu) \quad (33)$$

σ is a new length constant, the value of K will be large and σ will be small for a tightly coupled intracellular and extracellular spaces.

Using Eq. (33) in Eq. (31) we get

$$\frac{B\upsilon}{\sigma^3}\sin h\left(\frac{y}{\sigma}\right) = K\left(2Ay + \frac{B}{\sigma}sin\ h\left(\frac{y}{\sigma}\right) - 2Ay - \frac{-\frac{\upsilon}{\mu}\mathrm{B}}{\sigma}sin\ h\left(\frac{y}{\sigma}\right)\right)$$

$$\frac{B\upsilon}{\sigma^3}sin\ h\left(\frac{y}{\sigma}\right) = K\left(\frac{B}{\sigma}sin\ h\left(\frac{y}{\sigma}\right) + \frac{\upsilon\mathrm{B}}{\mu\sigma}sin\ h\left(\frac{y}{\sigma}\right)\right),$$

$$\frac{B\upsilon}{\sigma^3}sin\ h\left(\frac{y}{\sigma}\right) = K\frac{B}{\sigma}sin\ h\left(\frac{y}{\sigma}\right)\left(1+\frac{\upsilon}{\mu}\right)$$

$$\frac{B\upsilon}{\sigma^3}sin\ h\left(\frac{y}{\sigma}\right) = K\frac{B}{\sigma}sin\ h\left(\frac{y}{\sigma}\right)\left(\frac{\mu+\upsilon}{\mu}\right) \quad (34)$$

$$\frac{B\upsilon}{\sigma^3}sin\ h\left(\frac{y}{\sigma}\right) = \frac{B}{\sigma}sin\ h\left(\frac{y}{\sigma}\right)\upsilon\left(\frac{1}{\frac{\upsilon\mu}{K(\mu+\upsilon)}}\right)$$

$$\frac{B\upsilon}{\sigma^3}sin\ h\left(\frac{y}{\sigma}\right) = \frac{B\upsilon}{\sigma}sin\ h\left(\frac{y}{\sigma}\right)\left(\frac{1}{\sigma^2}\right)$$

$$\frac{B\upsilon}{\sigma^3}sin\ h\left(\frac{y}{\sigma}\right) = \frac{B\upsilon}{\sigma^3}sin\ h\left(\frac{y}{\sigma}\right)$$

Similarly using Eq. (33) in Eq. (32) we get

$$\frac{D\mu}{\sigma^3}\sin h\left(\frac{y}{\sigma}\right) = -K\left(2Ay + \frac{B}{\sigma}sin\ h\left(\frac{y}{\sigma}\right) - 2Ay - \frac{-\frac{\upsilon}{\mu}\mathrm{B}}{\sigma}sin\ h\left(\frac{y}{\sigma}\right)\right)$$

$$\frac{B\upsilon}{\sigma^3}sin\ h\left(\frac{y}{\sigma}\right) = -K\left(\frac{B}{\sigma}sin\ h\left(\frac{y}{\sigma}\right) + \frac{\upsilon\mathrm{B}}{\mu\sigma}sin\ h\left(\frac{y}{\sigma}\right)\right)$$

$$\frac{B\upsilon}{\sigma^3}sin\ h\left(\frac{y}{\sigma}\right) = -K\frac{B}{\sigma}sin\ h\left(\frac{y}{\sigma}\right)\left(1+\frac{\upsilon}{\mu}\right)$$

$$\frac{B\upsilon}{\sigma^3}sin\ h\left(\frac{y}{\sigma}\right) = -K\frac{B}{\sigma}sin\ h\left(\frac{y}{\sigma}\right)\left(\frac{\mu+\upsilon}{\mu}\right) \quad (35)$$

$$\frac{B\upsilon}{\sigma^3}sin\ h\left(\frac{y}{\sigma}\right) = -\frac{B}{\sigma}sin\ h\left(\frac{y}{\sigma}\right)\upsilon\left(\frac{1}{\frac{\upsilon\mu}{K(\mu+\upsilon)}}\right)$$

$$\frac{B\upsilon}{\sigma^3}sin\ h\left(\frac{y}{\sigma}\right) = -\frac{B\upsilon}{\sigma}sin\ h\left(\frac{y}{\sigma}\right)\left(\frac{1}{\sigma^2}\right)$$

$$\frac{B\upsilon}{\sigma^3}sin\ h\left(\frac{y}{\sigma}\right) = -\frac{B\upsilon}{\sigma^3}sinh\left(\frac{y}{\sigma}\right)$$

4.2 Boundary conditions

In order to find the value of unknown involving in equations we should apply a boundary conditions at $y = L$ and $y = -L$ the stresses $\tau_{ixx} = \tau_{ixy} = \tau_{exx} = \tau_{eyy} = 0$. At the surface boundary conditions are $\tau_{ixy} = 0$ and $\tau_{exy} = \pm \mathrm{F}$. These boundary conditions are helpful to determine the values of unknowns. In order to prove $\tau_{ixx} = \tau_{ixy} = \tau_{exx} = \tau_{eyy} = 0$ we take

$$\tau_{ixx} = -p + 2\upsilon\varepsilon_{ixx} + \gamma\varepsilon_{ixx} + T$$

$$\tau_{ixx} = -p + 2\upsilon\left(\frac{\partial u_x}{\partial x}\right) + \gamma\left(\left(\frac{\partial u_x}{\partial x}\right) + T,\right.$$

$$\tau_{ixx} = -p + 2\upsilon\frac{\partial}{\partial x}\left(\frac{\partial\phi}{\partial y}\right) + \gamma\frac{\partial}{\partial x}\left(-\frac{\partial\phi}{\partial x}\right) + T$$

$$\tau_{ixx} = -p + 2\upsilon\frac{\partial^2\phi}{\partial x\partial y} - \gamma\frac{\partial^2\phi}{\partial x^2} + T$$

$$\tau_{ixx} = 0 + 2\upsilon(0) - \gamma(0) + 0$$

$$\tau_{ixx} = 0$$

Similarly

$$\tau_{iyy} = -p + 2\upsilon\varepsilon_{iyy}$$

$$\tau_{iyy} = -p + 2\upsilon\left(\frac{\partial u_x}{\partial x}\right)$$

$$\tau_{iyy} = 0 + 2\upsilon\frac{\partial}{\partial y}\left(-\frac{\partial\phi}{\partial x}\right)$$

$$\tau_{iyy} = 0 - 2\upsilon\frac{\partial^2\phi}{\partial x\partial y}$$

$$\tau_{iyy} = 0 - 2\upsilon(0)$$

$$\tau_{iyy} = 0.$$

For

$$\tau_{exx} = -q + 2\mu\varepsilon_{exx}$$
$$\tau_{exx} = -q + 2\mu\left(\frac{\partial w_x}{\partial x}\right)$$
$$\tau_{exx} = 0 + 2\mu\frac{\partial}{\partial x}\left(\frac{\partial \eta}{\partial y}\right)$$
$$\tau_{exx} = 0 + 2\mu\frac{\partial^2 \eta}{\partial x \partial y}$$
$$\tau_{exx} = 0 + 2\mu(0)$$
$$\tau_{exx} = 0$$

Similarly

$$\tau_{eyy} = -q + 2\mu\varepsilon_{eyy}$$
$$\tau_{eyy} = -q + 2\mu\left(\frac{\partial w_y}{\partial y}\right)$$
$$\tau_{eyy} = 0 + 2\mu\frac{\partial}{\partial y}\left(-\frac{\partial \eta}{\partial x}\right)$$
$$\tau_{eyy} = 0 - 2\mu\frac{\partial^2 \eta}{\partial x \partial y},$$
$$\tau_{eyy} = 0 - 2\mu(0)$$
$$\tau_{eyy} = 0$$

For

$$\tau_{ixy} = 0$$
$$\tau_{ixy} = 2\upsilon\varepsilon_{ixy}$$
$$\tau_{ixy} = 2\upsilon\left(\frac{1}{2}\left(\frac{\partial u_x}{\partial y} + \frac{\partial u_y}{\partial x}\right)\right)$$
$$\tau_{ixy} = \upsilon\left(\frac{\partial u_x}{\partial y} + \frac{\partial u_y}{\partial x}\right)$$
$$\tau_{ixy} = \upsilon\left(\frac{\partial}{\partial y}\left(\frac{\partial \phi}{\partial y}\right) + \frac{\partial}{\partial x}\left(-\frac{\partial \phi}{\partial x}\right)\right)$$
$$\tau_{ixy} = \upsilon\left(\frac{\partial^2 \phi}{\partial y^2} - \frac{\partial^2 \phi}{\partial x^2}\right)$$
$$\tau_{ixy} = \upsilon\left(\frac{\partial^2 \phi}{\partial y^2} - 0\right)$$
$$\tau_{ixy} = \upsilon\left(\frac{\partial^2 \phi}{\partial y^2}\right)$$
$$\tau_{ixy} = \upsilon\left(2A + \frac{B}{\sigma^2}cos\ h\left(\frac{y}{\sigma}\right)\right)$$
$$\tau_{ixy} = 2A\upsilon + \frac{B\upsilon}{\sigma^2}cos\ h\left(\frac{y}{\sigma}\right)$$
$$0 = 2A\upsilon + \frac{B\upsilon}{\sigma^2}cos\ h\left(\frac{y}{\sigma}\right) \quad (36)$$

For

$$\tau_{exy} = \pm F$$
$$\tau_{exy} = 2\mu\varepsilon_{exy}$$
$$\tau_{exy} = 2\mu\left(\frac{1}{2}\left(\frac{\partial w_x}{\partial y} + \frac{\partial w_y}{\partial x}\right)\right)$$
$$\tau_{exy} = \mu\left(\frac{\partial w_x}{\partial y} + \frac{\partial w_y}{\partial x}\right)$$
$$\tau_{exy} = \mu\left(\frac{\partial}{\partial y}\left(\frac{\partial \eta}{\partial y}\right) + \frac{\partial}{\partial x}\left(-\frac{\partial \eta}{\partial x}\right)\right)$$
$$\tau_{exy} = \mu\left(\frac{\partial^2 \eta}{\partial y^2} - \frac{\partial^2 \eta}{\partial x^2}\right)$$
$$\tau_{exy} = \mu\left(\frac{\partial^2 \phi}{\partial y^2} - 0\right)$$
$$\tau_{exy} = \mu\left(\frac{\partial^2 \phi}{\partial y^2}\right)$$
$$\tau_{exy} = \mu\left(2C + \frac{D}{\sigma^2}cos\ h\left(\frac{y}{\sigma}\right)\right)$$
$$\tau_{exy} = 2C\mu + cos\ h\left(\frac{y}{\sigma}\right)\frac{D\mu}{\sigma^2}$$
$$F = 2C\mu + cos\ h\left(\frac{L}{\sigma}\right)\frac{D\mu}{\sigma^2}$$
$$F = 2A\mu - \frac{\nu B}{\sigma^2}cos\ h\left(\frac{L\phi}{\sigma}\right) \quad (37)$$

Adding Eqs. (36) and (37) we get.

$$F = 2A\nu + 2A\mu$$
$$A = \frac{F}{2(\nu + \mu)} \quad (38)$$

Now subtracting Eqs. (36) and (37) we get

$$-F = \frac{2\nu B}{\sigma^2}cos\ h\left(\frac{L}{\sigma}\right) + 2A(\nu - \mu)$$

Using value of

$$\text{A} = \frac{F}{2(\nu+\mu)} \ ,$$
$$-F = \frac{2\nu B}{\sigma^2}\cos h\left(\frac{L}{\sigma}\right) + \frac{F(\nu-\mu)}{(\nu+\mu)}$$
$$-F - \frac{F(\nu-\mu)}{(\nu+\mu)} = \frac{2\nu B}{\sigma^2}\cos h\left(\frac{L}{\sigma}\right)$$
$$-F\left(\frac{\nu+\mu+\nu-\mu}{(\nu+\mu)}\right) = \frac{2\nu B}{\sigma^2}\cos h\left(\frac{L}{\sigma}\right)$$
$$-F\left(\frac{2\nu}{(\nu+\mu)}\right) = \frac{2\nu B}{\sigma^2}cos\ h\left(\frac{L}{\sigma}\right)$$
$$\frac{-\text{F}}{\nu+\mu}\frac{B}{\sigma^2} = cos\ h\left(\frac{L}{\sigma}\right)$$
$$B = \frac{-\text{F}\sigma^2}{(\nu+\mu)cos\ h\left(\frac{L}{\sigma}\right)} \quad (39)$$

Using Eqs. (38) and (39) in Eqs. (23) and (24) respectively we get

$$\phi = \frac{F}{\nu+\mu}\left(\frac{y^2}{2} - \sigma^2\frac{cos\ h\left(\frac{y}{\sigma}\right)}{cos\ h\left(\frac{L}{\sigma}\right)}\right) \quad (40)$$

and

$$\eta = \frac{F}{\nu+\mu}\left(\frac{y^2}{2} + \frac{\upsilon\sigma^2}{\mu}\frac{\cos h\left(\frac{y}{\sigma}\right)}{\cos h\left(\frac{L}{\sigma}\right)}\right) \quad (41)$$

The resulting displacements are

$$u_x = \frac{F}{\nu+\mu}\left(y - \sigma\frac{\sin h\left(\frac{y}{\sigma}\right)}{\cos h\left(\frac{L}{\sigma}\right)}\right) \quad (42)$$

$$u_y = 0 \quad (43)$$

$$w_x = \frac{F}{\nu+\mu}\left(y + \frac{\nu}{\mu}\sigma\frac{\sin h\left(\frac{y}{\sigma}\right)}{\cos h\left(\frac{L}{\sigma}\right)}\right) \quad (44)$$

$$w_y = 0 \quad (45)$$

$$\text{and } u_x - w_x = \frac{-F\sigma}{\mu}\frac{\sin h\left(\frac{y}{\sigma}\right)}{\cos h\left(\frac{L}{\sigma}\right)} \quad (46)$$

The strain for intracellular and extracellular region is

$$\varepsilon_{ixy} = \frac{F}{2(\nu+\mu)}\left(1 - \sigma\frac{\cos h\left(\frac{y}{\sigma}\right)}{\cos h\left(\frac{L}{\sigma}\right)}\right) \quad (47)$$

$$\varepsilon_{exy} = \frac{F}{2(\nu+\mu)}\left(1 + \frac{\nu}{\mu}\frac{\cos h\left(\frac{y}{\sigma}\right)}{\cos h\left(\frac{L}{\sigma}\right)}\right) \quad (48)$$

5. Result and discussion

The strain and stress are shown in Figs. 2 and 3 respectively. Throughout most of the kidney tissues, include near the center, the stress and strain are nearly constant. They vary near the edge of the kidney tissues in such a way τ_{ixx} and τ_{exx} go to zero at the boundary ($y = \pm L$). If the stress and strain are responsible for mechanotransduction then large effects would be seen at the center of the kidney tissues. The mechanical Bi domain model makes three novel predictions about the elastic properties of kidney tissues. First the differences between medulla and cortex displacements has a very different distribution then the two displacements individually Fig. 1. There are large displacements in the medulla but they are nearly the same in both spaces. Second large stresses and strain exist in the medulla region Figs. 2 and 3, whereas large differences exist in the displacement primarily at the boundary Fig. 1. The mechanical Bi domain model is based on hypothesis that differences in the displacement are responsible for mechanotransduction. The idea of this hypothesis is that integrin respond when they are stretched, and they are only stretched when the displacement in the medulla and cortex are different. If the two spaces each undergo complicated displacements, but the displacements are the same in both spaces. The predictions in Figs. 1-3, provide a way to test his hypothesis experimentally by measuring if mechano-

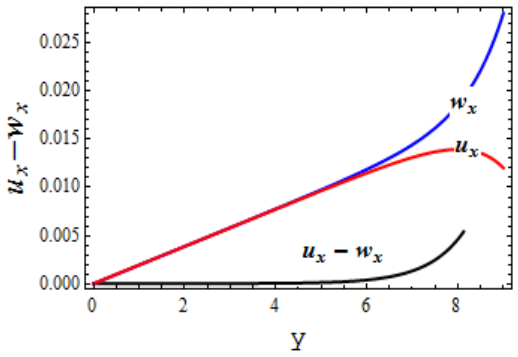

Fig. 1 Plot for intercellular and extracellular displacement differences when $F = -0.1, L = 8, \mu = 17.35, \nu = 34.25$

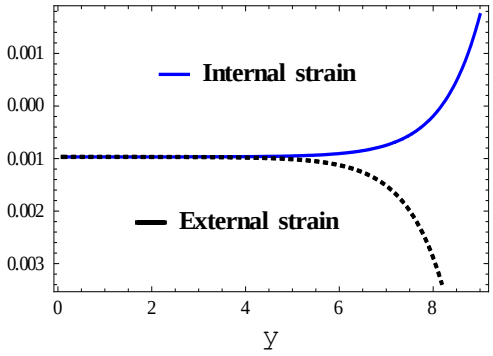

Fig. 2 Plot for intercellular and extracellular strain when $F = -0.1, L = 6, \mu = 17.35, \nu = 34.25$

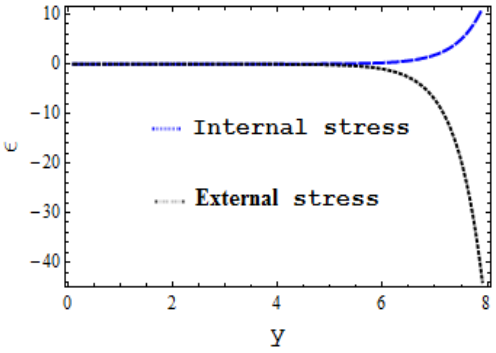

Fig. 3 Plot for intercellular and extracellular stress when $F = -0.1, L = 6, \mu = 17.35, \nu = 34.25$

transduction occurs where the stress and strain are large or where the difference in displacement is large. Third the model predicts how the length constant σ depends on the shear moduli υ and μ and the integrin constant density K.

Finally, they observed larger traction forces near the edge of the kidney tissue compared to the interior. If we take our integrin force, $K(u_x - w_x)$, as analogous to the traction force, then we too predict a larger force near the periphery. Our results are consistent with previous analyses based on the mechanical Bi domain model. For instance, when a tissue sheet is sheared the resulting expressions for the intracellular and extracellular displacements each contain two terms: a monodomain term that is common to both spaces and a Bi domain term that is responsible for forces on integrins. If $\sigma \ll L$, then the monodomain term

is larger than the Bi domain term, so measurements of tissue displacement are dominated by the monodomain term (Fig. 1). Experimental recordings of medulla and cortex displacements would need to be extremely precise in order to measure accurately their small difference. Moreover, the monodomain term implies that both the intracellular and extracellular spaces experience large, nearly uniform strains (Figs. 2 and 3). If one adopted the hypothesis that the intracellular stress or strain causes stem cell differentiation, one would expect differentiation to be distributed throughout the kidney tissues. However, if one adopts the hypothesis that the difference between the medulla and cortex displacements drives differentiation, then the model predicts that differentiation is confined to the edge of the kidney tissues.

6. Concluding remarks

The mechanical bidomain model is used to study the mechanical behavior of kidney tissues. This model has been used widely to study cardiac tissue and cell colony.

• On recognizing same structural and somehow same physiological relationship between cardiac tissue and kidney tissue, it is tried to analyze the displacements in different regions of kidney and the integrin, i.e., nephron coupling the intracellular medulla and extracellular cortex.

• The mechanical Bidomain model provides a microscopic description of kidney tissue mechanics

• The mechanical Bidomain model also predicts the microscopic coupling of extracellular cells region of kidney tissue, i.e., cortex and the intracellular cells region medulla of kidney.

Declaration of conflicting interests

The author(s) declared no potential conflicts of interest with respect to the research, authorship, and/or publication of this article.

Acknowledgement

This project was supported by the Deanship of Scientific Research at Prince Sattam Bin Abdulaziz University under the research project No 16794/01/2020.

References

Akbaş, Ş.D. (2016a), "Forced vibration analysis of viscoelastic nanobeams embedded in an elastic medium", *Smart Struct. Syst.*, **18**(6), 1125-1143. http://doi.org/10.12989/sss.2016.18.6.1125.

Akbaş, Ş.D. (2016b), "Analytical solutions for static bending of edge cracked micro beams", *Struct. Eng. Mech.*, **59**(3), 579-599. http://doi.org/10.12989/sem.2016.59.3.579.

Akbaş Ş.D. (2017a), "Free vibration of edge cracked functionally graded microscale beams based on the modified couple stress theory", *Int. J. Struct. Stabil. Dyn.*, **17**(3), 1750033. https://doi.org/10.1142/S021945541750033X.

Akbaş, Ş.D. (2017b), "Forced vibration analysis of functionally graded nanobeams", *Int. J. Appl. Mech.*, **9**(7), 1750100. https://doi.org/10.1142/S1758825117501009.

Akbaş, Ş.D. (2018a), "Forced vibration analysis of cracked functionally graded microbeams", *Adv. Nano Res.*, **6**(1), 39-55. http://doi.org/10.12989/anr.2018.6.1.039.

Akbaş, Ş.D. (2018b), "Bending of a cracked functionally graded nanobeam", *Adv. Nano Res.*, **6**(3), 219-243. http://doi.org/10.12989/anr.2018.6.3.219.

Akbaş, Ş.D. (2018c), "Forced vibration analysis of cracked nanobeams", *J. Brazil. Soc. Mech. Sci. Eng.*, **40**(8), 1-11. https://doi.org/10.1007/s40430-018-1315-1.

Arefi, M. and Zur, K.K. (2020), "Free vibration analysis of functionally graded cylindrical nanoshells resting on Pasternak foundation based on two-dimensional analysis", *Steel Compos. Struct.*, **34**(4), 615-623. http://doi.org/10.12989/scs.2020.34.4.615.

Benmansour, D.L., Kaci, A., Bousahla, A.A., Heireche, H., Tounsi, A., Alwabli, A.S., Alhebshi, A.M., Al-ghmady, K., Mahmoud, S.R. (2019), "The nano scale bending and dynamic properties of isolated protein microtubules based on modified strain gradient theory", *Adv. Nano Res.*, **7**(6), 443. http://doi.org/10.12989/anr.2019.7.6.443.

Civalek, Ö., Dastjerdi, S., Akbaş, Ş.D. and Akgöz, B. (2021), "Vibration analysis of carbon nanotube-reinforced composite microbeams", *Math. Method Appl. Sci.* https://doi.org/10.1002/mma.7069.

Eaton, H. (1992), "Electric field induced in a spherical volume conductor from arbitrary coils: Application to magnetic stimulation and MEG", *Med. Biol. Eng. Comput.*, **30**(4), 433-440. https://doi.org/10.1007/BF02446182.

Ebrahimi, F., Dabbagh, A., Rabczuk, T. and Tornabene, F. (2019), "Analysis of propagation characteristics of elastic waves in heterogeneous nanobeams employing a new two-step porosity-dependent homogenization scheme", *Adv. Nano Res.*, **7**(2), 135-143. https://doi.org/10.12989/anr.2019.7.2.135.

Eltaher, M.A., Almalki, T.A., Ahmed, K.I. and Almitani, K.H. (2019), "Characterization and behaviors of single walled carbon nanotube by equivalent-continuum mechanics approach", *Adv. Nano Res.*, **7**(1), 39-49. https://doi.org/10.12989/anr.2019.7.1.039.

Galappaththige, S.K., Gray, R.A. and Roth, B.J. (2017), "Cardiac strength-interval curves calculated using a bidomain tissue with a parsimonious ionic current", *PloS one*, **12**(2), e0171144. https://doi.org/10.1371/journal.pone.

Geselowitz, D.B. and Miller, W. (1983), "A bidomain model for anisotropic cardiac muscle", *Ann. Biomed. Eng.*, **11**(3-4), 191-206. https://doi.org/10.1007/BF02363286.

Gonzalez-Rosende, E., Jones, R.A., Sepulveda-Arques, J. and Zaballos-Garcia, E. (1988), "Pyrrole Studies. Part 40.1 Synthesis of 2-and 3-Substitoted 1-Methylindoles from Vinylpyrroles", *Synthetic Commun.*, **18**(14), 1669-1678. https://doi.org/10.1081/SCC-120003638.

Henriquez, C.S. and Ying, W. (2009), *The Bidomain Model of Cardiac Tissue: From Microscale to Macroscale Cardiac Bioelectric Therapy* in *Cardiac Bioelectric Therapy*, Springer, New York, U.S.A.

Karami, B. and Janghorban, M. (2020), "On the mechanics of functionally graded nanoshells", *Int. J. Eng. Sci.*, **153**, 103309. https://doi.org/10.1016/j.ijengsci.2020.103309.

Krassowska, W. and Neu, J.C. (1994), "Effective boundary conditions for syncytial tissues", *IEEE T. Biomed. Eng.*, **41**(2), 143-150. http://doi.org/10.1109/10.284925.

Leibovic, K.N. (2013), *Information Processing in The Nervous System: Proceedings of a Symposium held at the State University of New York at Buffalo 21st–24th October, 1968*, Springer Science & Business Media., Berlin, Germany.

Nazemnezhad, R. and Shokrollahi, H. (2020), "Free axial vibration of cracked axially functionally graded nanoscale rods incorporating surface effect", *Steel Compos. Struct.*, **35**(3), 449-462. http://doi.org/10.12989/scs.2020.35.3.449

Nejadi, M.M. and Mohammadimehr, M. (2020), "Buckling analysis of nano composite sandwich Euler-Bernoulli beam considering porosity distribution on elastic foundation using DQM", *Adv. Nano Res.*, **8**(1), 59-68. http://doi.org/10.12989/anr.2020.8.1.059.

Neu, J. and Krassowska, W. (1993), "Homogenization of syncytial tissues. Critical reviews in biomedical engineering", **21**(2), 137-199.

Neunlist, M. and Tung, L. (1995), "Spatial distribution of cardiac transmembrane potentials around an extracellular electrode: dependence on fiber orientation", *Biophys J.*, **68**(6), 2310-2322. http://doi.org/10.1016/s0006-3495(*95*)80413-3.

Noroozi, R., Barati, A., Kazemi, A., Norouzi, S. and Hadi, A. (2020), "Torsional vibration analysis of bi-directional FG nano-cone with arbitrary cross-section based on nonlocal strain gradient elasticity", *Adv. Nano Res.*, **8**(1), 13-24. https://doi.org/10.12989/anr.2020.8.1.013

Pathmanathan, P., Bernabeu, M.O., Bordas, R., Cooper, J., Garny, A., Pitt-Francis, J.M., Whiteley, J.P. and Gavaghan, D.J. (2010), "A numerical guide to the solution of the bidomain equations of cardiac electrophysiology", *Prog. Biophysics Mol. Bio.*, **102**(2-3), 136-155. http://doi.org/10.1016/j.pbiomolbio.2010.05.006.

Prior, P. and Roth, B.J. (2008), "Calculation of optical signal using three-dimensional bidomain/diffusion model reveals distortion of the transmembrane potential", *Biophys. J.*, **95**(4), 2097-2102. http://doi.org/10.1529/biophysj.107.127852.

Puwal, S. and Roth, B.J. (2010), "Mechanical bidomain model of cardiac tissue", *Phys. Rev. E*, **82**(4), 041904. http://doi.org/10.1103/PhysRevE.82.041904.

Roth, B.J. (1991), "Action potential propagation in a thick strand of cardiac muscle", *Circ. Res.*, **68**(1), 162-173. https://doi.org/10.1161/01.

Roth, B.J. (1992), "How the anisotropy of the intracellular and extracellular conductivities influences stimulation of cardiac muscle", *J. Math. Biol.*, **30**(6), 633-646. https://doi.org/10.1007/BF00175610.

Roth, B.J. (1996), "Strength-interval curves for cardiac tissue predicted using the bidomain model", *J. Cardiovasc. Electr.*, **7**(8), 722-737. http://doi.org/10.1111/j.1540-8167.1996.tb00580.x.

Roth, B.J. (2013), "The mechanical bidomain model: A review", *Int. Scholar. Res. Notice*, 863689. http://doi.org/10.1155/*2013*/863689.

Roth, B.J. (2016), "A mathematical model of mechano-transduction", arXiv:1611.08287, Cornell University, New York, U.S.A.

Roth, B.J. and Basser, P.J. (2009), "Mechanical model of neural tissue displacement during Lorentz effect imaging", *Magn. Reson. Med.*, **61**(1), 59-64. http://doi.org/10.1002/mrm.21772.

Safaei, B., Khoda, F.H. and Fattahi, A.M. (2019), "Non-classical plate model for single-layered graphene sheet for axial buckling", *Adv. Nano. Res.*, **7**(4), 265-275. http://doi.org/10.12989/anr.2019.7.4.265.

Sepulveda, N.G., Roth, B.J. and Wikswo Jr, J.P. (1989), "Current injection into a two-dimensional anisotropic bidomain", *Biophys. J.*, **55**(5), 987-999. http://doi.org/10.1016/S0006-3495(*89*)82897-8.

Shahsavari, D., Karami, B. and Janghorban, M. (2019), "Size-dependent vibration analysis of laminated composite plates", *Adv. Nano. Res.*, **7**(5), 337-349. http://doi.org/10.12989/anr.2019.7.5.337.

Sharma, K. and Roth, B.J. (2014), "How compressibility influences the mechanical bidomain model", *Biomath*, **3**(2), 1411171. http://doi.org/10.11145/j.biomath.2014.11.171.

Supraja, N., Tollamadugu, N.V.K.V.P. and Adam, S. (2016), "Phytogenic silver nanoparticles (Alstonia scholaris) incorporated with epoxy coating on PVC materials and their biofilm degradation studies", *Adv. Nano. Res.*, **4**(4), 281-284. http://doi.org/10.12989/anr.2016.4.4.281

Trayanova, N.A., Roth, B.J. and Malden, L.J. (1993), "The response of a spherical heart to a uniform electric field: A bidomain analysis of cardiac stimulation", *IEEE T. Biomed. Eng.*, **40**(9), 899-908. http://doi.org/10.1109/10.245611.

Trayanova, N. and Plank, G. (2009), *Bidomain Model of Defibrillation* in *Cardiac Bioelectric Therapy*, Springer. New York, U.S.A.

Trayanova, N., Plank, G. and Rodríguez, B. (2006), "What have we learned from mathematical models of defibrillation and postshock arrhythmogenesis? Application of bidomain simulations", *Heart Rhythm*, **3**(10), 1232. http://doi.org/10.1016/j.hrthm.2006.04.

Tung, L. (1978), "A bi-domain model for describing ischemic myocardial dc potentials", Ph.D. Dissertation, Massachusetts Institute of Technology, Massachusetts, U.S.A.

Wikswo Jr, J.P., Lin, S.F. and Abbas, R.A. (1995), "Virtual electrodes in cardiac tissue: A common mechanism for anodal and cathodal stimulation", *Biophys. J.*, **69**(6), 2195-2210. http://doi.org/10.1016/S0006-3495(*95*)80115-3.

Zhou, C., Zhang, Z., Zhang, J., Fang, Y. and Tahouneh, V. (2020), "Vibration analysis of FG porous rectangular plates reinforced by graphene platelets", *Steel Compos. Struct.*, **34**(2), 215-226. http://doi.org/10.12989/scs.2020.34.2.215.

CC